

## THERMAL RADIATION EFFECT ON UNSTEADY MHD REAR STAGNATION POINT IN $Al_2O_3$ -Cu/ $H_2O$ HYBRID NANOFLUIDS

(Kesan Sinaran Haba pada Aliran Titik Genangan Belakang MHD tak Mantap dalam Nanobendalir Hibrid  $Al_2O_3$ -Cu/ $H_2O$ )

NURUL AMIRA ZAINAL\*, ISKANDAR WAINI, NAJIYAH SAFWA KHASHI'IE, ROSLINDA NAZAR & IOAN POP

### ABSTRACT

The evaluation of high thermal efficiency has garnered considerable interest in the context of the unique properties demonstrated by hybrid nanofluids. Therefore, the present study investigates the impact of heat radiation on the unsteady rear stagnation point magnetohydrodynamic (MHD) flow of hybrid nanofluids. The utilisation of similarity transformations allows for the conversion of differential equations with several variables into a specific class of ordinary differential equations. The mathematical model is solved with the *bvp4c* function. The findings suggest that the unsteady rear stagnation MHD flow in hybrid nanofluid exhibits enhanced heat transfer properties compared to both nanofluid types. The augmentation of nanoparticle concentration and the influence of suction are discovered to have a positive effect on the skin friction coefficient. As the thermal radiation parameter is elevated, a concomitant reduction in the rate of heat transmission is observed. Furthermore, the findings illustrate the presence of two distinct solutions within a particular range.

*Keywords:* stagnation point flow; MHD; hybrid nanofluid; thermal radiation; *bvp4c*

### ABSTRAK

Penilaian kecekapan haba yang tinggi telah mendapat perhatian yang signifikan berhubung dengan ciri-ciri berbeza yang dipamerkan oleh nanobendalir hibrid. Oleh yang demikian, kajian ini mengkaji kesan sinaran haba pada aliran titik genangan belakang magnetohidrodinamik (MHD) tak mantap dalam nanobendalir hibrid  $Al_2O_3$ -Cu/ $H_2O$ . Penggunaan penjelmaan keserupaan membolehkan penukaran persamaan pembezaan berbilang pemboleh ubah kepada persamaan pembezaan biasa. Model matematik yang telah ditentukan diselesaikan dengan menggunakan fungsi *bvp4c*. Keputusan menunjukkan bahawa aliran nanobendalir hibrid pada titik genangan belakang MHD diiktiraf mempunyai keupayaan pemindahan haba yang unggul berbanding dengan kedua-dua aliran nanobendalir. Peningkatan kepekatan nanozarah dan kesan sedutan diperhatikan dapat meningkatkan pekali geseran kulit. Apabila parameter sinaran haba meningkat, terdapat penurunan yang sepadan dalam kadar penghantaran haba. Di samping itu, keputusan kajian menunjukkan kewujudan penyelesaian dual dalam julat tertentu pada parameter meregang/mengecut.

*Kata kunci:* aliran titik genangan; MHD; nanobendalir hibrid; radiasi terma; *bvp4c*

## 1. Introduction

Based on prior investigations, the incorporation of nanoparticles into conventional fluids has been observed to augment their thermal conductivity, hence improving their heat transfer capabilities

(Suresh *et al.* 2011). Consequently, a novel heat transfer fluid has been developed. Hybrid nanofluids are a promising and innovative fluid category with significant potential for many industrial applications. Nanoparticles are dispersed inside conventional fluids to generate them. In addition, the formulation of these fluids may involve the incorporation of either metal or non-metal particles in order to get the most effective combination of the mixture. Hybrid nanofluids have been employed in diverse domains, encompassing heat transfer (Huminc & Huminc 2018; Sidik *et al.* 2016).

Nevertheless, the selection of suitable nanoparticles is a crucial determinant in maintaining the stability of hybrid nanofluids. Further evaluation of the flow and heat transfer in the boundary layer, considering different governing parameters within hybrid nanofluids can be found in the following studies. Khashi'ie *et al.* (2022) elucidate the comparative efficacy of heat absorption in relation to heat generation inside the thermal flow process of. Shoaib *et al.* (2020) conclude that an increased value of the magnetic parameter led to elevated levels of frictional forces, resulting in a reduction of the velocity field and an increase in the temperature field. In another study, Waini *et al.* (2022) suggest that the inclusion of the unsteadiness parameter produces a supporting influence on the rate of heat transfer, while Zainal *et al.* (2022) reached to conclusion that lowering the unsteadiness parameter proportionally increases the performance of the heat transfer.

According to Ajbar *et al.* (2023) experimental work, it was found that all hybrid nanofluids exhibit enhanced thermal efficiency in parabolic trough solar collectors. Alshuhail *et al.* (2023) deduce that most of the research concluded that boosting the collector's thermal efficiency can be achieved by replacing the working fluid with high thermal conductivity fluids known as nanofluids and hybrid nanofluids. This was found to be the case in most of the studies. Meanwhile, Modi *et al.* (2023) conducted comparative performance research on the utilisation of mono and hybrid nanofluids. The study revealed that the incorporation of nanoparticles into the base fluid enhances both the thermal characteristics and heat transfer capability.

Researchers have also shown considerable interest in the stagnation flow owing to its significant relevance in the field of engineering. The study conducted by Greco *et al.* (2020) significantly contributed to the analysis of flow management at the rear stagnation point. However, the focus of the previous research was on steady currents. Instability in the flow may occur if the free stream velocity or the surface temperature suddenly changes. The effect of buoyancy on the unsteady flow across a vertical surface was studied by Devi *et al.* (1991), using boundary layer approximations. Fang and Jing (2013) made significant findings by identifying exact solutions in the context of unsteady rear stagnation point flow. Recently, researchers have conducted analytical and numerical investigations on the phenomenon of unsteady flow. Analytical solutions to heat conduction issues with three different forms of periodic boundary conditions were discovered by Xu *et al.* (2023), along with applications of these solutions. In their study conducted in 2023, Yahaya *et al.* (2023) identified the presence of dual solutions throughout the computational process, instigating an investigation into the stability of the solution. The analysis correctly identified the first solution as stable and meaningful from a physical standpoint.

An analytical study conducted by Izadi *et al.* (2020) revealed that the use of the MHD parameter demonstrates a favourable influence on the thermal progression of nanofluids within porous metals, specifically for the purpose of cooling central processing units (CPUs). The findings align with the experimental investigation undertaken by Chen *et al.* (2021). In a separate

investigation, Mohyud-Din *et al.* (2018) conducted a comprehensive examination of a research endeavour focused on analysing the impact of heat and mass transfer on the magnetohydrodynamic (MHD) motion of nanoparticles. The employment of a magnetic field has been reported to enable the modification of boundary layer separation in several physical phenomena. In a study conducted by Waini *et al.* (2020), it was reported that the utilisation of a hybrid nanofluid, in the presence of a magnetic field, resulted in enhanced thermal performance when compared to a regular nanofluid. Several relevant studies pertaining to the aforementioned discourse are currently accessible, including those conducted by Jaafar *et al.* (2022), Wahid *et al.* (2022), and Zainal *et al.* (2021).

From the above literature reviews, the current study is intended to carefully evaluate the hybrid nanofluid with the combination of alumina/copper nanoparticles and a magnetic field subjected to an unsteady MHD rear stagnation point flow. The research emphasises the novelty of the conceptual hybrid model employed to address the unsteady flow problem, incorporating both MHD and thermal radiation effects. The comprehensive examination of the suggested model, particularly the mathematical framework of the hybrid nanofluid model in unsteady rear stagnation point flow with magnetic and thermal radiation impact, has not been comprehensively examined in previous scholarly investigations. The earlier study conducted by Turkyilmazoglu *et al.* (2017) and Bhattacharyya (2011) did not incorporate these particular features. Furthermore, this study has examined the outcomes of dual solutions in relation to the encompassing issue. Moreover, the examination of the impact of suction on boundary layer flow is subject to debate, thus necessitating an investigation of this particular parameter. The ultimate analysis is presented in the form of figures and tables. This research exhibits the utilisation of a quantitative approach in the thermal extrusion manufacturing procedure, particularly in the production of plastic films. The results of this study are expected to make a valuable contribution to the existing knowledge in the fields of thermal systems and boundary layer analysis, particularly for fellow scientists and researchers. The understanding of flow properties within the stagnation zone of the potential heat transfer fluid has significant practical ramifications, which makes it notably relevant.

## 2. Problem Formulation

The unsteady MHD rear stagnation-point flow of  $Al_2O_3-Cu/H_2O$  hybrid nanofluids with radiation impact past a permeable surface is considered, as demonstrated in Figure 1. The velocity is noted as  $u_\infty = -u_0x/(1-\xi t)$ , which  $u_0$  and  $\xi$  are constant, that calculate the unsteadiness strength. The wall's moving velocity is  $u_w = u_0x/(1-\xi t)$  and  $v_w(x, t)$  along the  $x$ - and  $y$ - axis, respectively. Further,  $T_w(x, t) = T_\infty + T_0x/L(1-\xi t)$  is wall temperature, while  $T_\infty$  is ambient temperature. It is stated that there is no variation in the size of the nanoparticles. On the basis of the aforementioned presumption, the governing equations of the mathematical model of hybrid nanofluids can be formulated as follows (Devi *et al.* 1991; Fang & Jing 2013):

$$\frac{\partial u}{\partial x} + \frac{\partial v}{\partial y} = 0, \quad (1)$$

$$\frac{\partial u}{\partial t} + u \frac{\partial u}{\partial x} + v \frac{\partial u}{\partial y} = \frac{\partial u_\infty}{\partial t} + u_\infty \frac{\partial u_\infty}{\partial x} + \frac{\mu_{mf}}{\rho_{mf}} \frac{\partial^2 u}{\partial y^2} - \frac{\sigma_{mf}}{\rho_{mf}} B_0^2 (u - u_\infty), \quad (2)$$

$$\frac{\partial T}{\partial t} + u \frac{\partial T}{\partial x} + v \frac{\partial T}{\partial y} = \frac{k_{hnf}}{(\rho C_p)_{hnf}} \frac{\partial^2 T}{\partial y^2} - \frac{1}{(\rho C_p)_{hnf}} \frac{\partial q_r}{\partial y}. \quad (3)$$

Next, using the Rosseland approximation, the radiative heat flux  $q_r$  is given by Rosseland (1936):

$$q_r = -\frac{4\sigma^*}{3k^*} \frac{\partial T^4}{\partial y}, \quad (4)$$

where  $\sigma^*$  is the Stefan-Boltzman constant and  $k^*$  is the mean absorption coefficient of the nanofluid. Now, we assume that the temperature difference within the flow is such that  $T^4$  may be expanded in Taylor's series. Thus, expanding  $T^4$  about  $T_\infty$  and neglecting the higher-order terms we get:

$$T^4 \cong 4T_\infty^3 T - 3T_\infty^4, \quad (5)$$

Hence, we have:

$$\frac{\partial q_r}{\partial y} = -\frac{16T_\infty^3 \sigma^*}{3k^*} \frac{\partial^2 T}{\partial y^2}. \quad (6)$$

Consequently, using Eq. (6) in Eq. (3) we obtain:

$$\frac{\partial T}{\partial t} + u \frac{\partial T}{\partial x} + v \frac{\partial T}{\partial y} = \frac{k_{hnf}}{(\rho C_p)_{hnf}} \frac{\partial^2 T}{\partial y^2} + \frac{16T_\infty^3 \sigma^*}{3k^* (\rho C_p)_{hnf}} \frac{\partial^2 T}{\partial y^2}. \quad (7)$$

Meanwhile, the boundary conditions of the above mathematical assumption are given by:

$$\begin{aligned} v = v_w(x,t), u = \lambda u_w(x,t), T = T_w(x,t), \quad \text{at } y = 0, \\ u \rightarrow u_\infty(x,t), T \rightarrow T_\infty(x), \quad \text{as } y \rightarrow \infty. \end{aligned} \quad (8)$$

The wall mass transfer  $v_w(x,t)$  denotes as  $v_w(x,t) < 0$  for suction, while  $B_0$  is the transverse magnetic. The shrinking parameter is symbolised by  $\lambda < 0$  while  $\lambda > 0$  represent stretching surface. Table 1 presents the physical features of the fluids that have been chosen for analysis. Meanwhile, Table 2 displays the correlation coefficient specifically for the hybrid nanofluids.

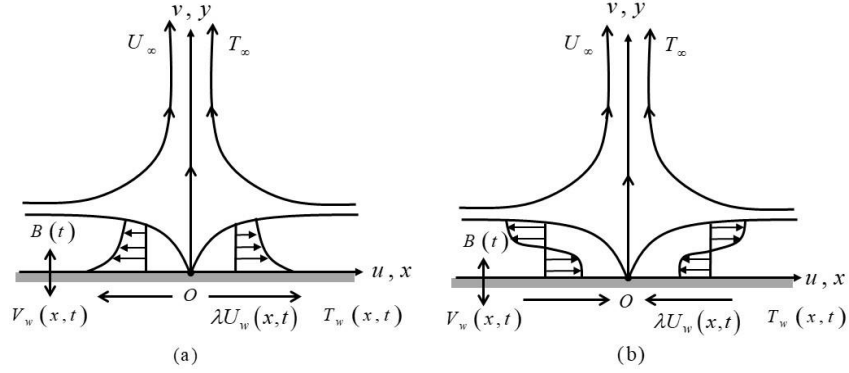


Figure 1: The coordinate systems of the mathematical model: (a) stretching (b) shrinking sheet

Table 1: Thermophysical properties of nanoparticles (Abu-Nada & Oztop 2009)

Physical properties	$\rho (kg / m^3)$	$k (W / mK)$	$C_p (J / kgK)$
H <sub>2</sub> O	997.1	0.613	4179
Al <sub>2</sub> O <sub>3</sub>	3970	40	765
Cu	8933	400	385

Table 2: The correlation coefficient of hybrid nanofluid (Takabi & Salehi 2014; Ghalambaz *et al.* 2020)

Properties	$Al_2O_3-Cu/H_2O$
Density	$\rho_{hnf} = (1 - \phi_{hnf})\rho_f + \phi_1\rho_{s1} + \phi_2\rho_{s2}$
Dynamic viscosity	$\mu_{hnf} = \mu_f / (1 - \phi_{hnf})^{2.5}$
Thermal capacity	$(\rho C_p)_{hnf} = (\rho C_p)_f (1 - \phi_{hnf}) + (\rho C_p)_{s1} \phi_1 + (\rho C_p)_{s2} \phi_2$
Thermal conductivity	$\frac{k_{hnf}}{k_f} = \left[ \frac{\left( \frac{k_{s1}\phi_1 + k_{s2}\phi_2}{\phi_{hnf}} \right) + 2k_f + 2(k_{s1}\phi_1 + k_{s2}\phi_2) - 2k_f\phi_{hnf}}{\left( \frac{k_{s1}\phi_1 + k_{s2}\phi_2}{\phi_{hnf}} \right) + 2k_f - (k_{s1}\phi_1 + k_{s2}\phi_2) + k_f\phi_{hnf}} \right]$
Electrical conductivity	$\frac{\sigma_{hnf}}{\sigma_f} = \left[ \frac{\left( \frac{\phi_1\sigma_{s1} + \phi_2\sigma_{s2}}{\phi_{hnf}} \right) + 2\sigma_f + 2(\phi_1\sigma_{s1} + \phi_2\sigma_{s2}) - 2\phi_{hnf}\sigma_f}{\left( \frac{\phi_1\sigma_{s1} + \phi_2\sigma_{s2}}{\phi_{hnf}} \right) + 2\sigma_f - (\phi_1\sigma_{s1} + \phi_2\sigma_{s2}) + \phi_{hnf}\sigma_f} \right]$

The following similarity variables are implemented (Fang & Jing 2013):

$$\psi(x, y, t) = \sqrt{\frac{u_0 \nu_f}{(1-\xi t)}} x f(\eta), \quad \eta = \sqrt{\frac{u_0}{(1-\xi t) \nu_f}} y, \quad \theta(\eta) = \frac{T - T_\infty}{T_w - T_\infty}, \quad (9)$$

thus,

$$u = \frac{u_0 x f'(\eta)}{(1-\xi t)}, \quad v = -\sqrt{\frac{u_0 \nu_f}{(1-\xi t)}} f(\eta), \quad v_w = -\sqrt{\frac{u_0 \nu_f}{(1-\xi t)}} S, \quad (10)$$

Next, by invoking the similarity variables in Eqs. (9) and (10), so we have:

$$\frac{\mu_{mf}/\mu_f}{\rho_{mf}/\rho_f} f''' + ff'' - f'^2 + 1 - \zeta \left( f' + \frac{\eta}{2} f'' + 1 \right) - \frac{\sigma_{mf}/\sigma_f}{\rho_{mf}/\rho_f} M (f' + 1) = 0, \quad (11)$$

$$\frac{1}{\text{Pr}} \left( \frac{1}{(\rho C_p)_{mf}/(\rho C_p)_f} \right) \left( \frac{k_{mf}}{k_f} + \frac{4}{3} Rd \right) \theta'' + f \theta' - f' \theta - \zeta \left( \theta + \frac{\eta}{2} \theta' \right) = 0, \quad (12)$$

$$\begin{aligned} f(0) &= S, \quad f'(0) = \lambda, \quad \theta(0) = 1, \\ f'(\eta) &\rightarrow -1, \quad \theta(\eta) \rightarrow 0, \end{aligned} \quad (13)$$

which  $M = \sigma_f B / u_0 \rho_f$  corresponds to the magnetic parameter where  $B = B_0 \sqrt{1 - \xi t}$ ,  $\text{Pr} = \mu_f C_p / k_f$ , and  $\zeta = \xi / a$  is the unsteady parameter. The radiation parameter is denoted as  $Rd = 4\sigma^* T_\infty^3 / k_f k^*$ . The necessary physical quantities are

$$Nu_x = \frac{x}{k_f (T_w - T_\infty)} \left[ -k_{mf} \left( \frac{\partial T}{\partial y} \right)_{y=0} + (q_r)_{y=0} \right]$$

and

$$C_f = \frac{\mu_{mf}}{\rho_f u_\infty^2} \left( \frac{\partial u}{\partial y} \right)_{y=0}.$$

Then, we have:

$$\text{Re}_x^{1/2} C_f = \frac{\mu_{mf}}{\mu_f} f''(0), \quad \text{Re}_x^{-1/2} Nu_x = - \left( \frac{k_{mf}}{k_f} + \frac{4}{3} Rd \right) \theta'(0), \quad (14)$$

where  $Re_x = u_0 x^2 / \nu_f (1 - \xi t)$ .

### 3. Results Interpretation

This section documents the results of the computation of Eqs. (11)-(13) using the bvp4c proposed in the earlier conceptual framework. A relative tolerance value of  $10^{-10}$  is utilised in the implemented computation. In the given scenario, it is necessary to make an initial assumption for Eqs. (11)-(13) when utilising the bvp4c tool, as there is a potential for multiple (dual) solutions. Although the predictive capabilities of the bvp4c technique are limited, it has the potential to ultimately achieve convergence towards the intended initial solution. Hence, the process of determining a suitable first estimate for the initial solution is uncomplicated. Nevertheless, the challenge of identifying an alternative solution that satisfies the requirements of being a suitably precise approximation is quite arduous. In this specific instance, the utilisation of the continuation approach was employed, as suggested by Shampine *et al.* (2003). The study's validity is substantiated through a comparative analysis with previous studies. The discoveries and findings presented in Table 3 exhibit a noteworthy level of consistency. Table 3 presents a comparison between the outcomes of the current viscous fluid model and those obtained by Bhattacharyya (2011) and Turkyilmazoglu *et al.* (2017). Additionally, it is crucial to emphasise the existence of many solutions in Figures 2–5. These solutions can be attributed to the satisfaction of the boundary condition in Eq. (13) provided the parameter values are employed within the designated range.

Table 3. Approximation values of  $Re_x^{1/2} C_f$  as  $\varepsilon = M = \delta = S = \phi_1 = \phi_2 = 0$ .

$\lambda$	Present result		Bhattacharyya 2011		Turkyilmazoglu <i>et al.</i> 2017	
	First sol.	Second sol.	First sol.	Second sol.	First sol.	Second sol.
-0.25	1.4022408	-	1.4022405	-	1.4022408	-
-0.50	1.4956698	-	1.4956697	-	1.4956670	-
-0.75	1.4892982	-	1.4892981	-	1.4892982	-
-1.00	1.3288169	0.0000000	1.3288169	0.0000000	1.3288168	0.0000000
-1.15	1.0822312	0.1167021	1.0822316	0.1167023	1.0822312	0.1167021
-1.20	0.9324733	0.2336497	0.9324728	0.2336491	0.9324733	0.2336497
-1.2465	0.5842817	0.5542962	0.5842915	0.5542856	0.5842813	0.5542947
-1.24657	0.5745257	0.5640125	0.5745268	0.5639987	0.5774525	0.5640081

Various physical parameters employed in this investigation were numerically calculated. In this investigation, we use several variants of  $\phi$  i.e.  $0.00 \leq \phi_1, \phi_2 \leq 0.01$ . The domain of nanoparticle concentrations explored in this work is based on the empirical inquiry undertaken by Suresh *et al.* (2011; 2012). The researchers conducted a study in which they synthesised and characterised a nanocomposite powder consisting of  $Al_2O_3$ -Cu/water. They investigated several volume concentrations of the nanocomposite, between 0.1% to 2%. The authors conducted a study to assess the stability of the nanofluids they prepared. This was achieved by measuring the pH of the nanofluids. The findings of the study revealed a negative correlation between the volume concentration of nanofluids and their stability. Therefore, we have reached the conclusion that the hybrid nanofluid, which involves the suspension of different nanoparticles such as alumina ( $Al_2O_3$ ) and copper (Cu) in water, holds great potential for yielding substantial insights into the study of boundary layer flow and heat transfer properties in the present examination. According

to Turkyilmazoglu (2015), it has been shown that nanofluids exhibit non-Newtonian fluid behaviour when their volumetric concentration surpasses a range of 5% to 6%. Consequently, the selection of the total amount of copper nanoparticles and alumina nanoparticles in this investigation adheres to the specified range of  $0.01 \leq \lambda \leq 0.02$  volume fraction.

Additionally, a variety of controlling parameter values are defined to the preceding scope where the value of the magnetic and unsteadiness parameter are fixed to  $M = 6.0$ ,  $\zeta = -2.0$ , while the suction and radiation parameter are set within  $3.0 \leq S \leq 4.0$  and  $0.0 \leq Rd \leq 0.5$ , respectively, in order to ensure that the results achieved are compatible with one another. It is important to note that an adequate preliminary estimation needs to be determined by the values of the provided parameter in order to get the desired solution. In the entire study, the dual solutions are observed with a particular range of a critical point, i.e.,  $\lambda_c$  only when the sheet is shrinking ( $\lambda < 0$ ). Meanwhile, no solution is observed when  $\lambda < \lambda_c$  as it describes the occurrence of the boundary layer separation.

Figure 2 describes the influence of nanoparticles concentration when  $\phi$  is varied as the sheet shrinks. When  $\phi_1 = 0.00, \phi_2 = 0.01$ , the alumina-water nanofluid ( $\text{Al}_2\text{O}_3/\text{H}_2\text{O}$ ) is formed, while  $\phi_1 = 0.01, \phi_2 = 0.00$  denoted the copper-water nanofluid ( $\text{Cu}/\text{H}_2\text{O}$ ). The combination of  $\phi_1 = \phi_2 = 0.01$  produced the alumina-copper/water hybrid nanofluids ( $\text{Al}_2\text{O}_3 - \text{Cu}/\text{H}_2\text{O}$ ). As shown in Figure 2(a), the increment of  $\phi$  evidently improves the trend in the skin friction coefficient ( $f''(0)$ ) when applied to a shrinking surface. The result indicates that the combination of  $\text{Al}_2\text{O}_3 - \text{Cu}/\text{H}_2\text{O}$  presented the highest trend in  $f''(0)$  followed by  $\text{Cu}/\text{H}_2\text{O}$  and  $\text{Al}_2\text{O}_3/\text{H}_2\text{O}$ . This may be due to the frictional drag exerted upsurges and potentially slowing the boundary layer separation on the shrinking surface of  $\text{Al}_2\text{O}_3 - \text{Cu}/\text{H}_2\text{O}$ . The increase in the rate of heat transfer  $-\theta'(0)$  corresponds to the increment of  $\phi$  is accessible in Figure 2(b). All fluids are seen to fluctuate upside down along the shrinking sheet. The combination of several parameter including the radiation parameter may contribute to this diversity of flow characteristic. Focusing on the highest peak of the flow trend, it is proven that the  $\text{Al}_2\text{O}_3 - \text{Cu}/\text{H}_2\text{O}$  shows better performance in heat transfer efficiency. The data presented in the figure indicates that the rate of heat transfer in the alumina-water nanofluid ( $\text{Al}_2\text{O}_3/\text{H}_2\text{O}$ ) is comparatively lower than that observed in the copper-water nanofluid ( $\text{Cu}/\text{H}_2\text{O}$ ). In aluminium nanoparticles, free electrons are more likely to be scattered by phonons than in copper nanoparticles. Hence, copper have better heat and electrical conductivity which make copper is a better conductor than aluminium. However, aluminium is more flexible which makes it easier to wind in production. In order to optimise the individual behaviour of the nanoparticles, the researcher has implemented a hybrid nanofluid to enhance the thermo-rheological features of the single particle nanofluids. As a result, it can be observed that the hybrid nanofluid exhibits improved thermal conductivity and excellent dispersion stability due to the predominant attributes of individual nanoparticles.

Figures 3(a) and 3(b) depict the velocity profile  $f'(\eta)$  and temperature profile  $-\theta'(\eta)$ , respectively. Figure 3(a) apparently showed that the increasing values of nanoparticles volume concentration  $\phi$  specifically in  $\text{Al}_2\text{O}_3 - \text{Cu}/\text{H}_2\text{O}$ , increase the momentum boundary layer thickness in the first and second solutions. Meanwhile, the temperature distribution profile  $\theta(\eta)$  presents a downward trend with the addition of  $\phi$  in the shrinking surface, as exhibited in Figure 3(b). As can be seen, the thickness of the thermal boundary layer inclines in both solutions. In addition to that, the outcomes of Figure 3(b) is aligned with Figure 2(b) where the relation between the reduction of temperature profile distributions and heat transfer rate coefficient is



observed. Overall, both velocity and temperature distribution profiles met the far-field boundary conditions (13) asymptotically when  $\eta_\infty = 6$  is implemented. The impact of suction effect  $S$  in  $Al_2O_3-Cu/H_2O$  are portrayed in Figures 4(a) and 4(b) concerning  $f''(0)$  and  $-\theta'(0)$ , respectively. Figure 4(a) displays that as  $S$  improved,  $f''(0)$  increases in both solutions. On the other hand, Figure 4(b) illustrates an increasing pattern of  $-\theta'(0)$  when  $S$  improves in the first solution, hence we can conclude that the thermal performance quality has improved as the suction parameter enhances. The inclusion of suction is to simultaneously cause fluid motion to move quicker and assist hot particles in moving toward the wall, which speeds up heat transfer. Additionally, the increase in suction values has expanded the scope of potential solutions, as illustrated in Figure 4, hence allowing for a prolongation of the boundary layer separation phenomenon.

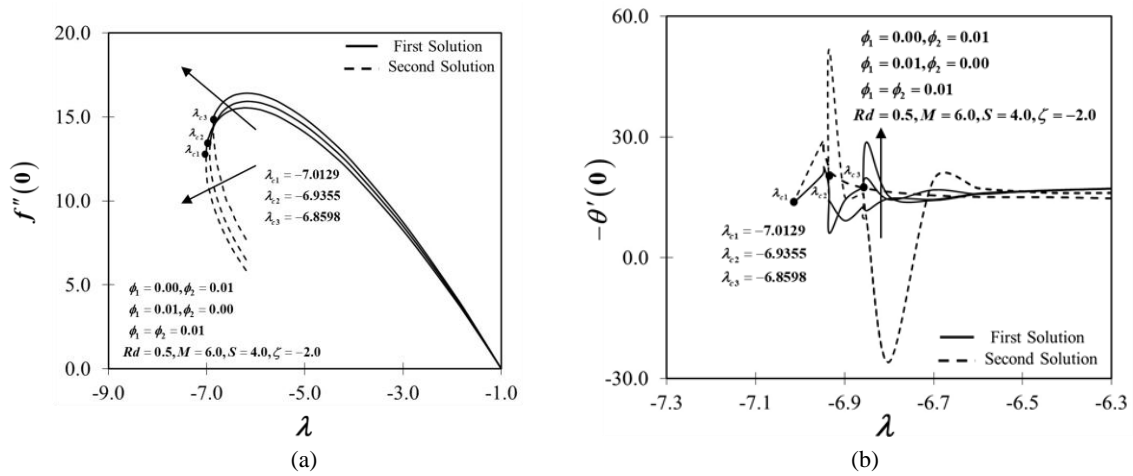


Figure 2: Different values of  $\phi$  versus  $\lambda$  (a) reduced skin friction coefficient (b) reduced heat transfer coefficient

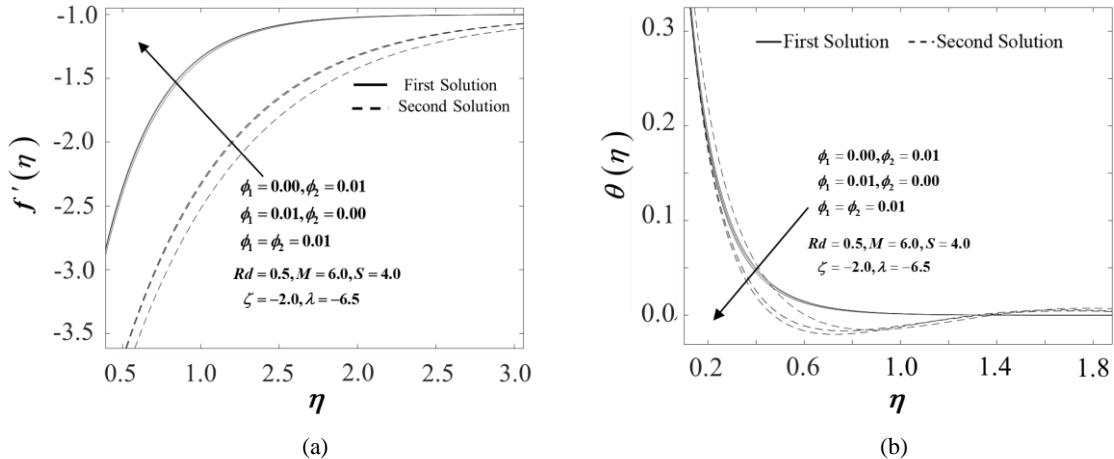


Figure 3: Different values of  $\phi$  with  $\eta$  (a) velocity profile (b) temperature profile

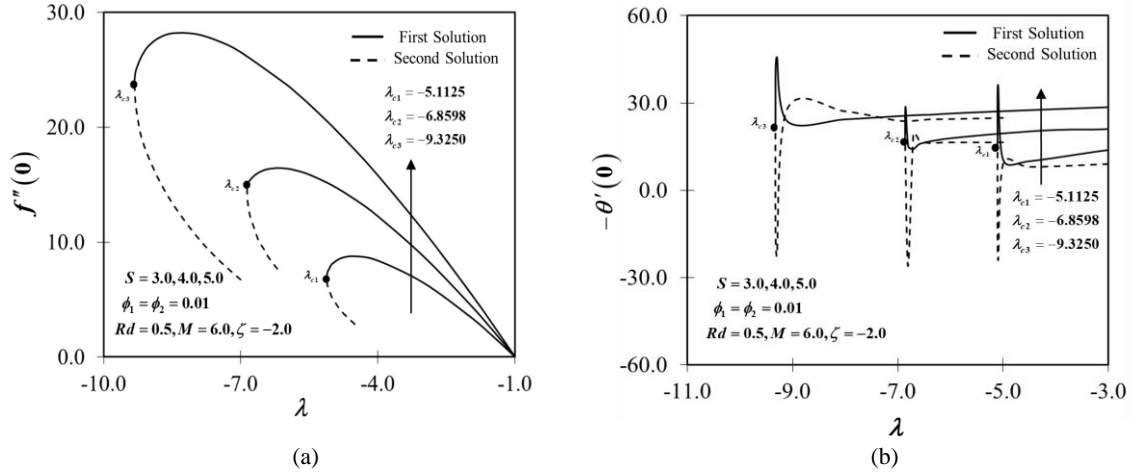


Figure 4. Different values of  $S$  with  $\lambda$  (a) reduced skin friction coefficient (b) reduced heat transfer coefficient

The influence of  $Rd$  is presented in Figure 5. Figure 5(a) shows the variations of  $-\theta'(0)$  for  $Rd = 0.0, 0.3, 0.5$ . Meanwhile,  $\theta(\eta)$  with respect to  $Rd$  is displayed in Figure 5(b). We found that  $Rd$  has a discernible effect on the temperature of the hybrid nanofluids that we were experimenting with. Physically,  $-\theta'(0)$  increases when  $Rd$  is increased as a result of the existence of thermal energy conversion, which also results in an increase in the thickness of the thermal boundary layer. This is because the presence of  $Rd$  causes a greater quantity of heat to be produced and released into the flow, which helps to increase the thickness of the momentum boundary layer. It is notable that the enhancement of the thermal field is due to a decrease in  $(k^*)$  as  $Rd$  increases. With the knowledge that the rate of energy transmission to the hybrid nanofluids is skewed due to the effect of  $Rd$ , the temperature of the fluids rises as  $Rd$  increases, as shown in Figure 5(b).

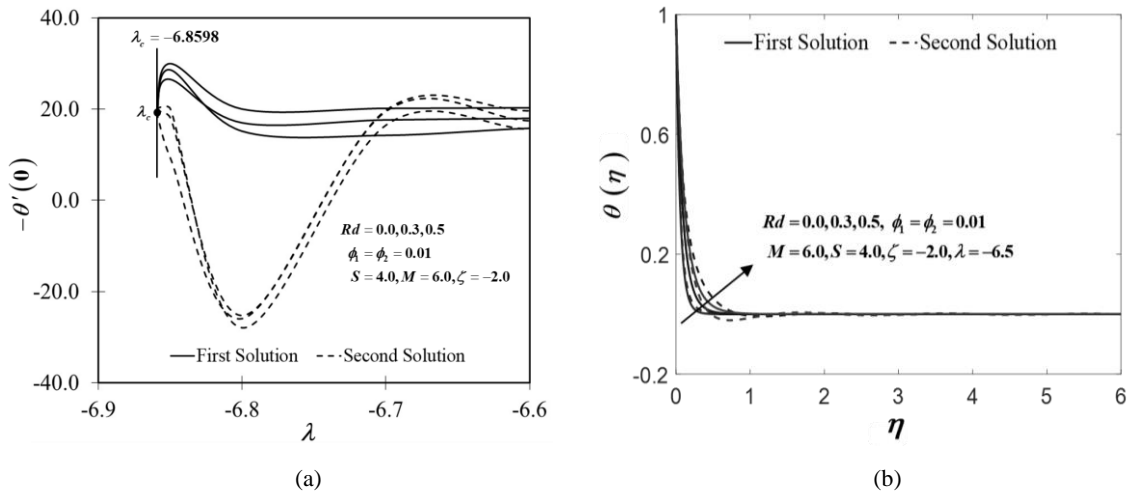


Figure 5. Different values of  $Rd$  with  $\lambda$  and  $\eta$  (a) velocity profile (b) temperature profile

#### 4. Conclusions

The present study aims to validate a computational model that simulates the effects of thermal radiation on the unsteady MHD flow at the rear stagnation point of a stretching or shrinking plate. Based on the data collected, it can be inferred that the existence of both the initial and following solutions is substantiated throughout a diverse spectrum of control parameters encompassing various nanoparticle configurations. It is apparent that enhancing the thermal efficiency can be achieved by the augmentation of both the concentration of nanoparticle volume fraction and the suction parameter. It can be observed that the thermal conductivity of Al<sub>2</sub>O<sub>3</sub>-Cu/H<sub>2</sub>O hybrid nanofluids is comparatively higher than that of traditional nanofluids, particularly when considering the suction parameter. In the context of the hybrid nanofluid system, an increase in radiation parameters leads to a decrease in thermal performance. This can be attributed to the excess heat generated by the conversion of thermal energy, which is then released into the working flow.

#### Acknowledgements

The present study is financially supported by GP-2021-K007136 granted by Universiti Kebangsaan Malaysia (UKM) and FRGS/1/2020/STG06/UKM/01/ provided by the Malaysian Ministry of Higher Education (MoHE). Also, the authors would like to acknowledge Universiti Teknikal Malaysia Melaka (UTeM) for the technical support.

#### References

- Abu-Nada E. & Oztop H.F. 2009. Effects of inclination angle on natural convection in enclosures filled with Cu–water nanofluid. *International Journal of Heat & Fluid Flow* **30**(4): 669-678.
- Ajbar W., Hernández J.A., Parrales A. & Torres L. 2023. Thermal efficiency improvement of parabolic trough solar collector using different kinds of hybrid nanofluids. *Case Studies in Thermal Engineering* **42**: 102759.
- Alshuhail L.A., Shaik F. & Sundar L.S. 2023. Thermal efficiency enhancement of mono and hybrid nanofluids in solar thermal applications—A review. *Alexandria Engineering Journal* **68**: 365-404.
- Bhattacharyya K. 2011. Dual solutions in boundary layer stagnation-point flow and mass transfer with chemical reaction past a stretching/shrinking sheet. *International Communications in Heat and Mass Transfer* **38**(7): 917-922.
- Chen T., Qi C., Tang J., Wang G. & Yan Y. 2021. Numerical and experimental study on optimization of CPU system cooled by nanofluids. *Case Studies in Thermal Engineering* **24**: 100848.
- Devi C.D.S., Takhar H.S. & Nath G. 1991. Unsteady mixed convection flow in stagnation region adjacent to a vertical surface. *Wärme-und Stoffübertragung* **26**(2): 71-79.
- Fang T. & Jing W. 2013. Closed-form analytical solutions of flow and heat transfer for an unsteady rear stagnation-point flow. *International Journal of Heat and Mass Transfer* **62**: 55-62.
- Ghalambaz M., Roşca N.C., Roşca A.V. & Pop I. 2020. Mixed convection and stability analysis of stagnation-point boundary layer flow and heat transfer of hybrid nanofluids over a vertical plate. *International Journal of Numerical Methods for Heat & Fluid Flow* **30**(7): 3737-3754.
- Greco C.S., Paolillo G., Astarita T. & Cardone G. 2020. The von Kármán street behind a circular cylinder: Flow control through synthetic jet placed at the rear stagnation point. *Journal of Fluid Mechanics* **901**: A39.
- Huminic G. & Huminic A. 2018. Hybrid nanofluids for heat transfer applications—a state-of-the-art review. *International Journal of Heat and Mass Transfer* **125**, 82-103.
- Izadi A., Siavashi M., Rasam H. & Xiong Q. 2020. MHD enhanced nanofluid mediated heat transfer in porous metal for CPU cooling. *Applied Thermal Engineering* **168**: 114843.
- Jaafar A., Waini I., Jamaludin A., Nazar R. & Pop I. 2022. MHD flow and heat transfer of a hybrid nanofluid past a nonlinear surface stretching/shrinking with effects of thermal radiation and suction. *Chinese Journal of Physics* **79**: 13–27.

- Khashi'ie N.S., Waini I., Zainal N.A., Hamzah K.B., Kasim A.R.M., Arifin N.M. & Pop I. 2022. Thermal progress of unsteady separated stagnation point flow with magnetic field and heat generation in hybrid ferrofluid. *Nanomaterials* **12**(18): 3205.
- Modi K.V., Patel P.R. & Patel S.K. 2023. Applicability of mono-nanofluid and hybrid-nanofluid as a technique to improve the performance of solar still: A critical review. *Journal of Cleaner Production* **387**: 135875.
- Mohyud-Din S.T., Khan U., Ahmed N. & Rashidi M.M. 2018. A study of heat and mass transfer on magnetohydrodynamic (MHD) flow of nanoparticles. *Propulsion and Power Research* **7**(1): 72–77.
- Rosseland S. 1936. *Theoretical Astrophysics*. Clarendon: Oxford University Press.
- Shampine L.F., Gladwell I. & Thompson S. 2003. *Solving ODEs with MATLAB*. Cambridge: Cambridge University Press.
- Shoaib M., Raja M.A.Z., Sabir M.T., Islam S., Shah Z., Kumam P. & Alrabaiah H. 2020. Numerical investigation for rotating flow of MHD hybrid nanofluid with thermal radiation over a stretching sheet. *Scientific Reports* **10**(1): 18533.
- Sidik N.A.C. Adamu I.M., Jamil M.M., Kefayati G.H.R. Mamat R. & Najafi G. 2016. Recent progress on hybrid nanofluids in heat transfer applications: A comprehensive review. *International Communications in Heat and Mass Transfer* **78**: 68-79.
- Suresh S., Venkataraj K.P. & Selvakumar P. 2011. Synthesis, characterisation of Al<sub>2</sub>O<sub>3</sub>-Cu nano composite powder and water based nanofluids. *Advanced Materials Research* **328-330**: 1560-1567.
- Suresh S., Venkataraj K.P., Selvakumar P. & Chandrasekar M. 2012. Effect of Al<sub>2</sub>O<sub>3</sub>-Cu/water hybrid nanofluid in heat transfer. *Experimental Thermal and Fluid Science* **38**: 54–60.
- Takabi B. & Salehi S. 2014. Augmentation of the heat transfer performance of a sinusoidal corrugated enclosure by employing hybrid nanofluid. *Advances in Mechanical Engineering* **6**: 147059.
- Turkyilmazoglu M. 2015. A note on the correspondence between certain nanofluid flows and standard fluid flows. *Journal of Heat Transfer* **137**(2): 024501.
- Turkyilmazoglu M., Naganthran K. & Pop I. 2017. Unsteady MHD rear stagnation-point flow over off-centred deformable surfaces. *International Journal of Numerical Methods for Heat & Fluid Flow* **27**(7): 1554-1570.
- Wahid N.S., Arifin N.M., Khashi'ie N.S., Pop I., Bachok N. & Hafidzuddin M.E.H. 2022. MHD mixed convection flow of a hybrid nanofluid past a permeable vertical flat plate with thermal radiation effect. *Alexandria Engineering Journal* **61**(4): 3323–3333.
- Waini I., Khashi'ie N.S., Kasim A.R.M., Zainal N.A., Hamzah K.B., Arifin N.M. & Pop I. 2022. Unsteady magnetohydrodynamics (MHD) flow of hybrid ferrofluid due to a rotating disk. *Mathematics* **10**(10): 1658.
- Waini I., Ishak A. & Pop I. 2020. MHD flow and heat transfer of a hybrid nanofluid past a permeable stretching/shrinking wedge. *Applied Mathematics and Mechanics* **41**(3): 507–520.
- Xu X., Li G., Zhao Y. & Liu T. 2023. Analytical solutions for heat conduction problems with three kinds of periodic boundary conditions and their applications. *Applied Mathematics and Computation* **442**: 127735.
- Yahaya R.I., Arifin N.M., Pop I., Ali F.M. & Isa S.S.P.M. 2023. Dual solutions of unsteady mixed convection hybrid nanofluid flow past a vertical riga plate with radiation effect. *Mathematics* **11**(1): 215.
- Zainal N.A., Nazar R., Naganthran K. & Pop I. 2022. Unsteady separated stagnation-point flow past a moving plate with suction effect in hybrid nanofluid. *Mathematics* **10**(11): 1933.
- Zainal N.A., Nazar R., Naganthran K. & Pop I. 2021. Unsteady MHD mixed convection flow in hybrid nanofluid at three- dimensional stagnation point. *Mathematics* **9**(5): 549.

Fakulti Teknologi dan Kejuruteraan Mekanikal  
Universiti Teknikal Malaysia Melaka  
76100 Durian Tunggal  
Melaka, MALAYSIA.  
Email: nurulamira@utem.edu.my\*, najiyah@utem.edu.my

Fakulti Teknologi dan Kejuruteraan Industri dan Pembuatan  
Universiti Teknikal Malaysia Melaka  
76100 Durian Tunggal  
Melaka, MALAYSIA.  
Email: iskandarwaini@utem.edu.my

*Department of Mathematical Sciences  
Faculty of Science and Technology  
Universiti Kebangsaan Malaysia  
43600 Bangi,  
Selangor, MALAYSIA.  
Email: [rmn@ukm.edu.my](mailto:rmn@ukm.edu.my)*

*Department of Mathematics  
Babeş-Bolyai University  
R-400084 Cluj-Napoca  
ROMANIA.  
Email: [popm.ioam@yahoo.co.uk](mailto:popm.ioam@yahoo.co.uk)*

Received: 17 July 2023

Accepted: 25 September 2023

---

<sup>†</sup>Corresponding author